

## Electronic supplementary information

Huiyeong Ju,<sup>a</sup> Honoka Tenma,<sup>a</sup> Miki Iwase,<sup>a</sup> Eunji Lee,<sup>a</sup> Mari Ikeda,<sup>c</sup> Shunsuke Kuwahara,<sup>ab</sup> Yoichi Habata<sup>\*ab</sup>

<sup>a</sup>Department of Chemistry and <sup>b</sup>Research Center for Integrated Properties, Faculty of Science, Toho University, 2-2-1 Miyama, Funabashi, Chiba 274-8510, Japan

<sup>c</sup>Department of Chemistry, Education Center, Faculty of Engineering, Chiba Institute of Technology, 2-1-1 Shibazono, Narashino, Chiba 275-0023, Japan

## Table of Contents

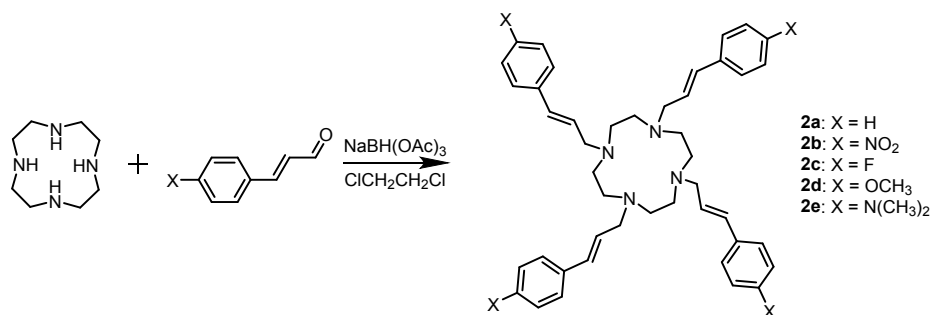
<b>Table S1</b> $[\alpha]_D$ of chiral alkyl nitriles .....	5
<b>Scheme S1</b> Synthesis of tetra-armed cyclens.....	5
<b>Fig. S1</b> $^1\text{H}$ and $^{13}\text{C}$ NMR spectra of <b>2a</b> .....	6
<b>Fig. S2</b> $^1\text{H}$ and $^{13}\text{C}$ NMR spectra of <b>2b</b> .....	7
<b>Fig. S3</b> $^1\text{H}$ and $^{13}\text{C}$ NMR spectra of <b>2c</b> .....	8
<b>Fig. S4</b> $^1\text{H}$ and $^{13}\text{C}$ NMR spectra of <b>2d</b> .....	9
<b>Fig. S5</b> $^1\text{H}$ and $^{13}\text{C}$ NMR spectra of <b>2e</b> .....	10
<b>Fig. S6</b> X-ray structure of <b>2a</b> , <b>2d</b> and <b>2e</b> .....	11
<b>Fig. S7</b> The interactions in <b>2e</b> molecules.....	11
<b>Fig. S8</b> The interactions in <b>2a</b> / $\text{Ag}^+$ complex .....	12
<b>Fig. S9</b> X-ray structure of <b>2b</b> / $\text{AgCF}_3\text{SO}_3$ .....	12
<b>Fig. S10</b> X-ray structure of <b>2c</b> / $\text{AgCF}_3\text{SO}_3$ .....	13
<b>Fig. S11</b> X-ray structure of <b>2a</b> / $\text{Cd}(\text{NO}_3)_2$ and <b>2a</b> / $\text{Co}(\text{NO}_3)_2$ .....	13
<b>Fig. S12</b> $\text{Ag}^+$ ion-induced $^1\text{H}$ NMR spectral changes of <b>2a</b> .....	14
<b>Fig. S13</b> $\text{Ag}^+$ ion-induced $^1\text{H}$ NMR spectral changes of <b>2b</b> .....	14
<b>Fig. S14</b> $\text{Ag}^+$ ion-induced $^1\text{H}$ NMR spectral changes of <b>2c</b> .....	15
<b>Fig. S15</b> $\text{Ag}^+$ ion-induced $^1\text{H}$ NMR spectral changes of <b>2d</b> .....	15
<b>Fig. S16</b> $\text{Ag}^+$ ion-induced $^1\text{H}$ NMR spectral changes of <b>2e</b> .....	16
<b>Fig. S17</b> Comparative $^1\text{H}$ NMR spectra of <b>2a</b> .....	16
<b>Fig. S18</b> Comparative $^1\text{H}$ NMR spectra of <b>1</b> .....	17
<b>Fig. S19</b> Acetonitrile-induced $^1\text{H}$ NMR spectral changes of <b>2a</b> / $\text{Ag}^+$ complex.....	17
<b>Fig. S20</b> Bulky nitrile-induced $^1\text{H}$ NMR spectral changes of <b>2a</b> / $\text{Ag}^+$ complex.....	18
<b>Table S2</b> Stability constants of acetonitrile and bulky nitrile guests with <b>2a</b> / $\text{Ag}^+$ .....	18
<b>Fig. S21</b> CD spectrum of chiral cyanohydrin ( <b>G6</b> ) ( $3.00 \times 10^{-3}\text{M}$ ).....	19
<b>Fig. S22</b> ( <i>S</i> )- <b>G1</b> and ( <i>R</i> )- <b>G1</b> -induced $^1\text{H}$ NMR spectral changes.....	20
<b>Fig. S23</b> HyperNMR output for <b>2a</b> / $\text{Ag}^+$ complex with ( <i>S</i> )- <b>G1</b> and ( <i>R</i> )- <b>G1</b> .....	21
<b>Fig. S24</b> Diffusion-ordered spectroscopy (DOSY) of <b>2a</b> / $\text{Ag}^+$ and ( <i>S</i> )- <b>G1</b> .....	21
<b>Fig. S25</b> Guest-induced CD and UV-vis changes for <b>2a</b> and another metal.....	22

<b>Fig. S26</b> Chiral nitriles-induced CD spectral changes of <b>2a</b> /Ag <sup>+</sup> complex.....	22
<b>Fig. S27</b> Chiral nitrile-induced <sup>1</sup> H NMR spectral changes of <b>2a</b> /Ag <sup>+</sup> complex .....	23
<b>Table S3</b> Stability constants of chiral nitrile guests with <b>2a</b> /Ag <sup>+</sup> complex.....	23
<b>Fig. S28</b> Structure of chiral amines as a guest ( <b>G7-G10</b> ).....	24
<b>Table S4</b> [α] <sub>D</sub> of chiral alkyl amines.....	24
<b>Fig. S29</b> CD spectra of <b>2a</b> /Ag <sup>+</sup> complex, chiral <b>G7</b> and chiral <b>G7@2a</b> /Ag <sup>+</sup> .....	25
<b>Fig. S30</b> CD spectra of <b>2a</b> /Ag <sup>+</sup> in presence of <b>G7</b> with various ee values.....	25
<b>Fig. S31</b> Chiral amines-induced CD spectral changes of <b>2a</b> /Ag <sup>+</sup> complex.....	26
<b>References</b> .....	26
<b>Table S5</b> Crystallographic Data and Structure Refinement.....	27
<b>Table S6</b> Selected Bond Lengths (Å) and Bond Angles (°) for <b>2a</b> /Ag.....	29
<b>Table S7</b> Selected Bond Lengths (Å) and Bond Angles (°) for <b>2a</b> /Cd.....	29
<b>Table S8</b> Selected Bond Lengths (Å) and Bond Angles (°) for <b>2a</b> /Co.....	30
<b>Table S9</b> Selected Bond Lengths (Å) and Bond Angles (°) for <b>2b</b> /Ag.....	30
<b>Table S10</b> Selected Bond Lengths (Å) and Bond Angles (°) for <b>2c</b> /Ag.....	30

**Table S1**  $[\alpha]_D$  of chiral alkyl nitriles

Compound	Temp. (°C)	$[\alpha]_D$	Compound	Temp. (°C)	$[\alpha]_D$
	20	+7.2 (c 3, CHCl <sub>3</sub> ) <sup>S1</sup>		20	+4.60 (c 5.09, CHCl <sub>3</sub> )
	20	-11 (neat) <sup>S2</sup>		*	+1.33 (c 1, CHCl <sub>3</sub> ) <sup>S3</sup>
	20	+37.5 (neat)		27.2	44.7 (c 1.03, CHCl <sub>3</sub> ) <sup>S4</sup>
	23	+8.79 (c 5.11, CHCl <sub>3</sub> )			

\*Temperature was not written in the reference.

**Scheme S1** Synthesis of tetra-armed cyclens with substituted styrylmethyl groups.

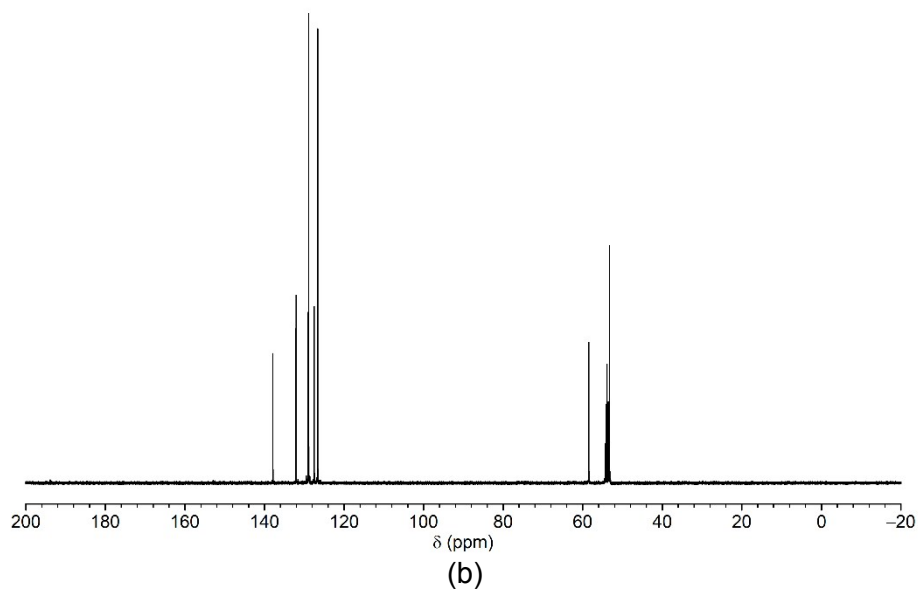
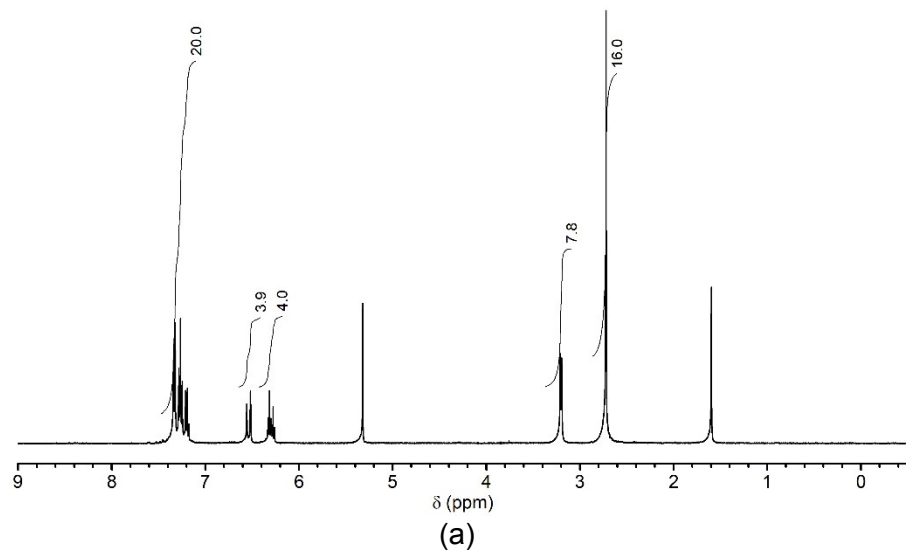


**Fig. S1** (a)  $^1\text{H}$  and (b)  $^{13}\text{C}$  NMR spectra of **2a** in  $\text{CD}_2\text{Cl}_2$ .

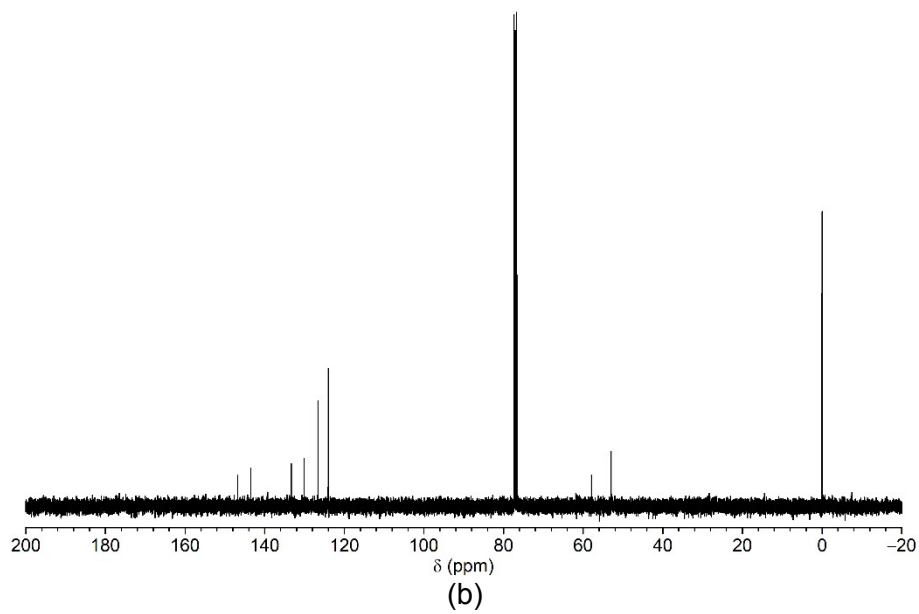
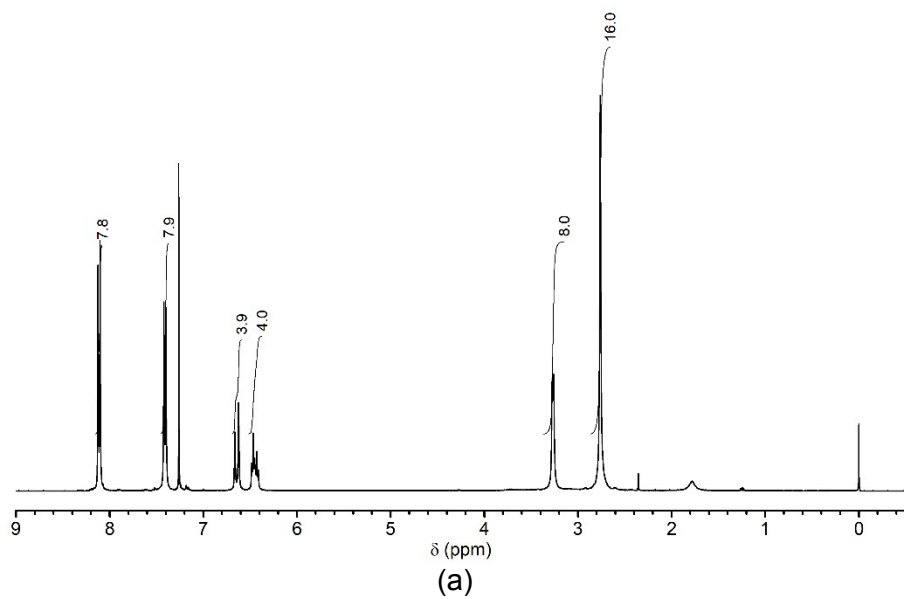


**Fig. S2** (a)  $^1\text{H}$  and (b)  $^{13}\text{C}$  NMR spectra of **2b** in  $\text{CDCl}_3$ .

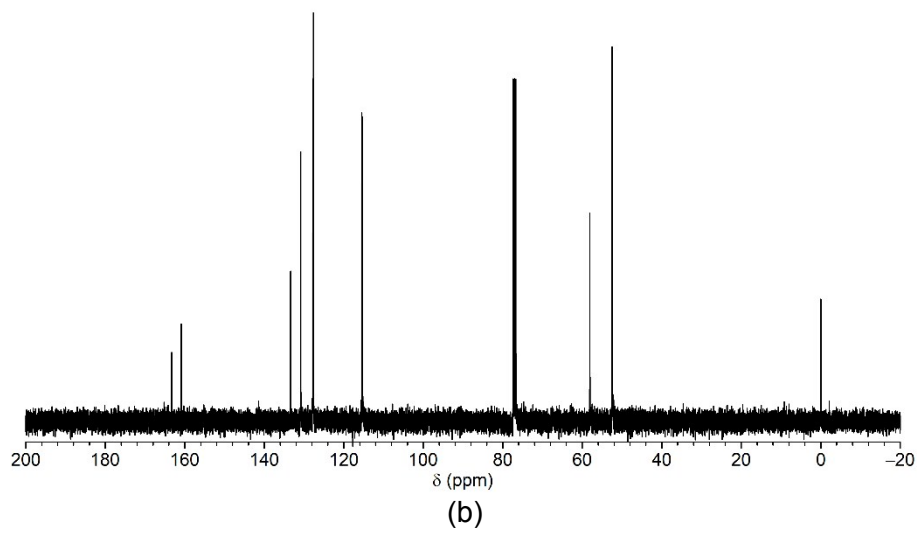
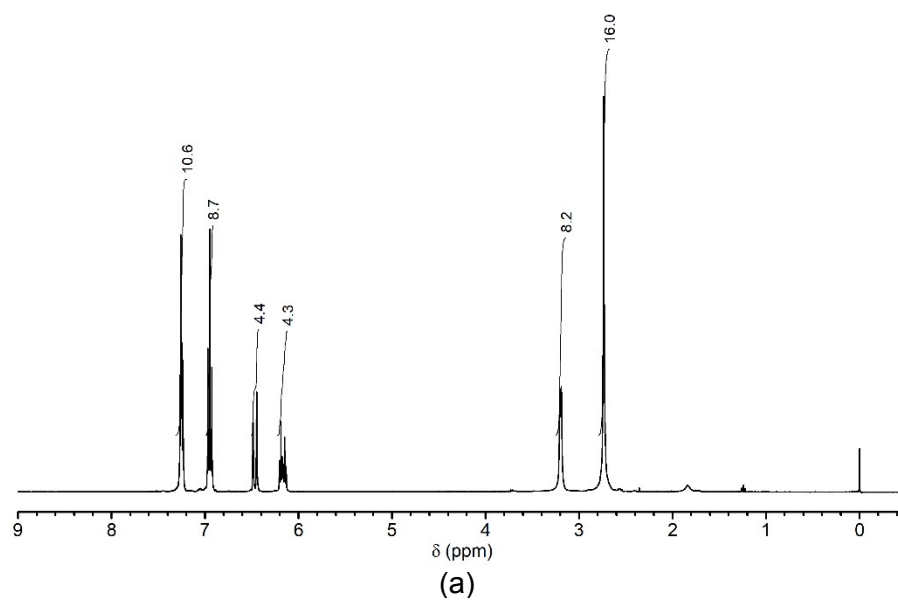


**Fig. S3** (a)  $^1\text{H}$  and (b)  $^{13}\text{C}$  NMR spectra of **2c** in  $\text{CDCl}_3$ .

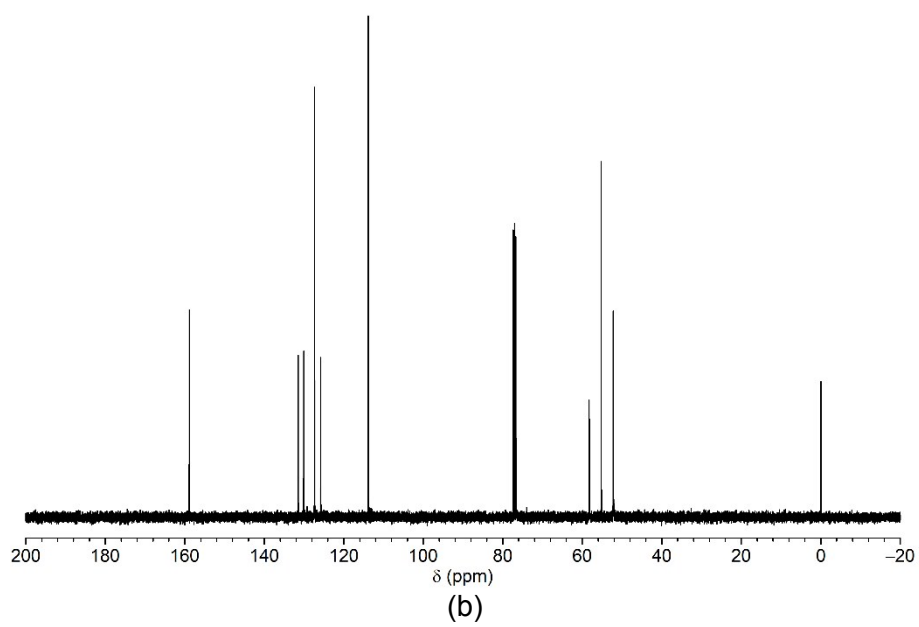
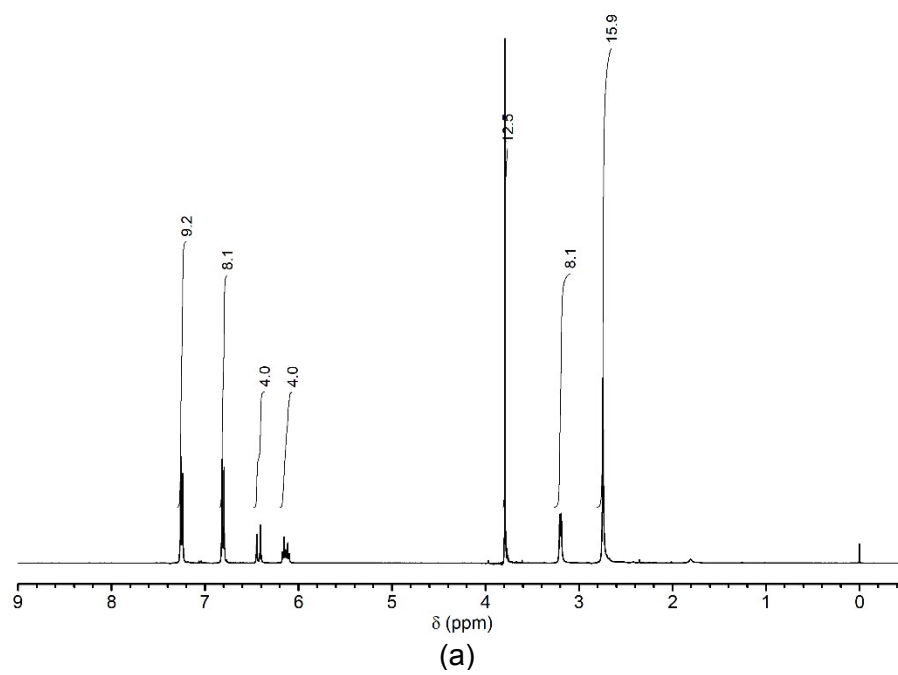


**Fig. S4** (a)  $^1\text{H}$  and (b)  $^{13}\text{C}$  NMR spectra of **2d** in  $\text{CDCl}_3$ .



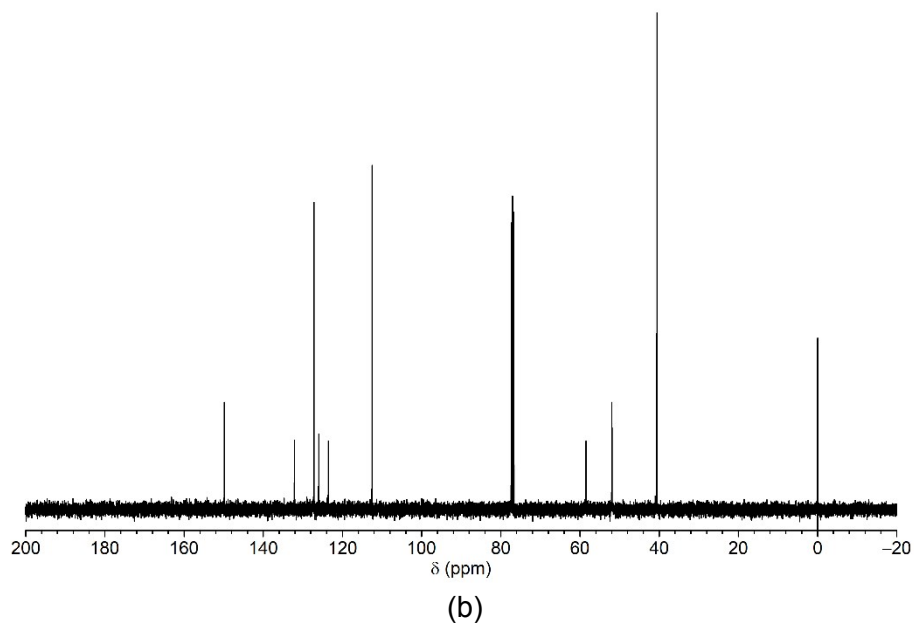
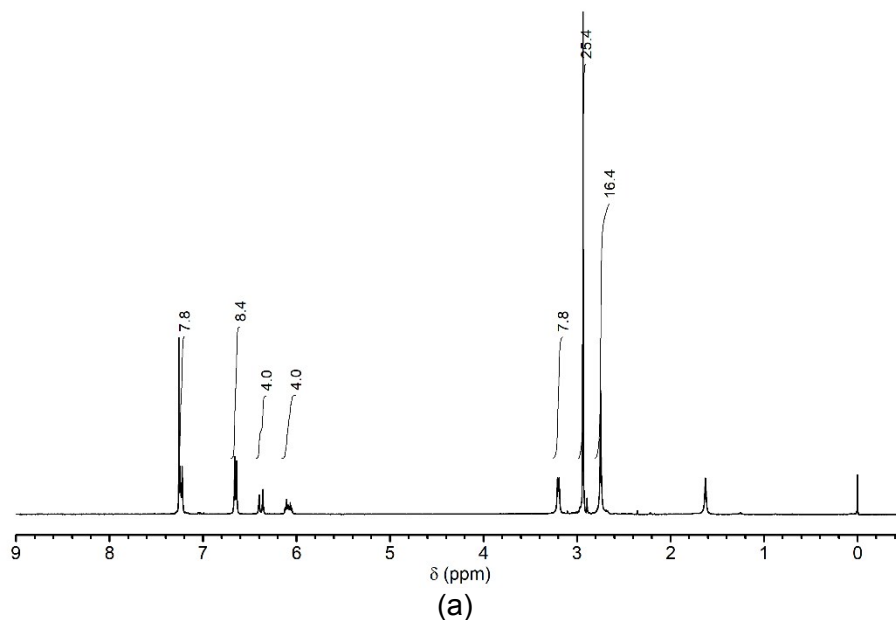


**Fig. S5** (a)  $^1\text{H}$  and (b)  $^{13}\text{C}$  NMR spectra of **2e** in  $\text{CDCl}_3$ .

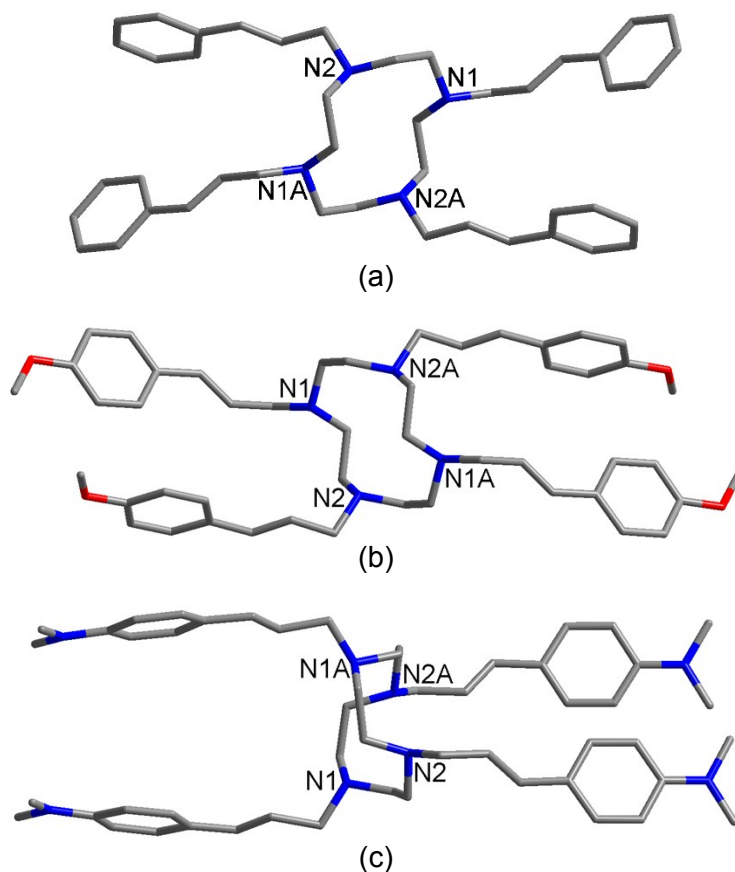


**Fig. S6** X-ray structure of (a) **2a**, (b) **2d** and (c) **2e**. Compounds **2a** and **2d** lies about an inversion centre. The asymmetric unit of **2e** has three half **2e** molecules, each lying about independent inversions centres. Difference-map plots (**2d** and **2e**) show that all methyl H atoms are correctly oriented. Hydrogen atoms omitted.

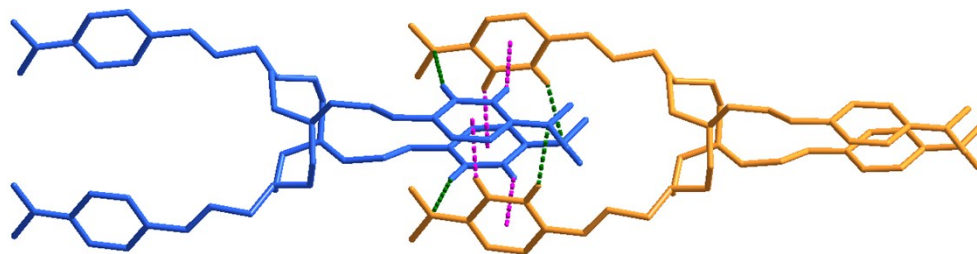


**Fig. S7** The interactions between two **2e** molecules; CH– $\pi$  interactions (pink dotted line, 2.771 and 2.774 Å) and (b) hydrogen bonds (green dotted line, 2.564 and 2.708 Å). Non-coordinated anions are omitted.

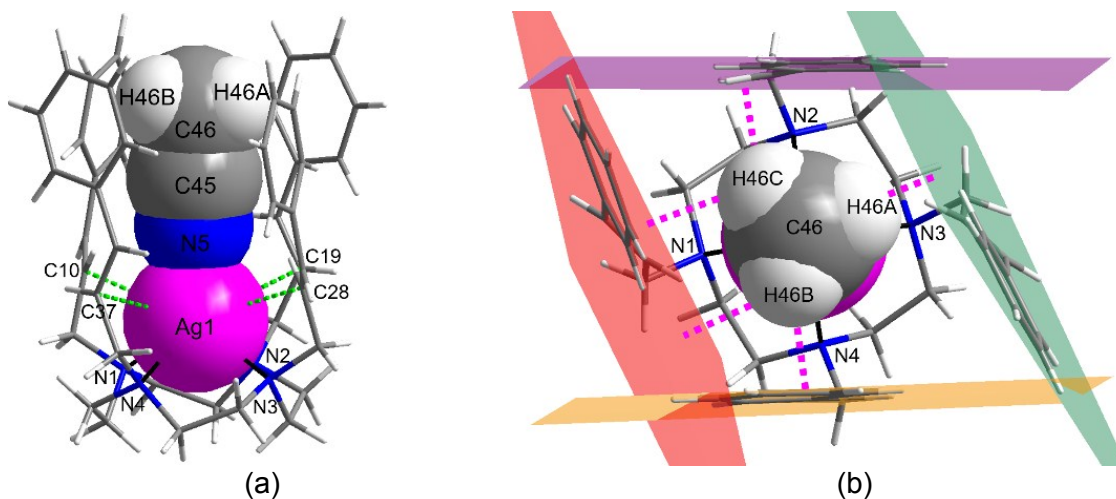


**Fig. S8** The interactions between (a)  $\text{Ag}^+$ - $\pi$  interaction (green dotted line) and (b)  $\text{H}_{\text{acetonitrile}^-}$ -benzene plane distances (pink dotted line) in **2a**/ $\text{Ag}^+$  complex. Non-coordinated anions are omitted.

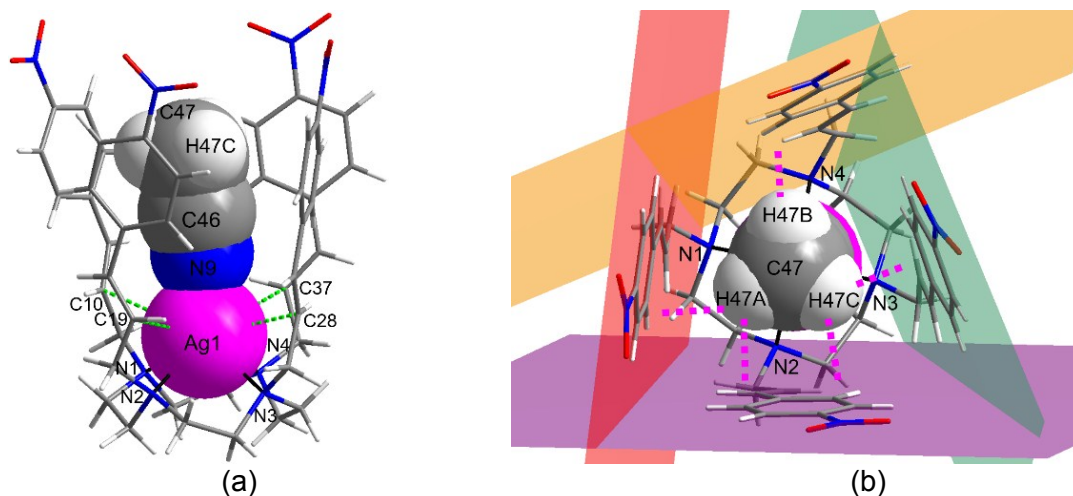


**Fig. S9** X-ray structure of **2b**/ $\text{AgCF}_3\text{SO}_3$ : (a) side view showing  $\text{Ag}^+$ - $\pi$  interaction (green dotted line) and (b) top view showing  $\text{H}_{\text{acetonitrile}^-}$ -benzene plane distances (pink dotted line). Difference-map plots show that the acetonitrile methyl H atoms are correctly oriented. Non-coordinated anions are omitted.

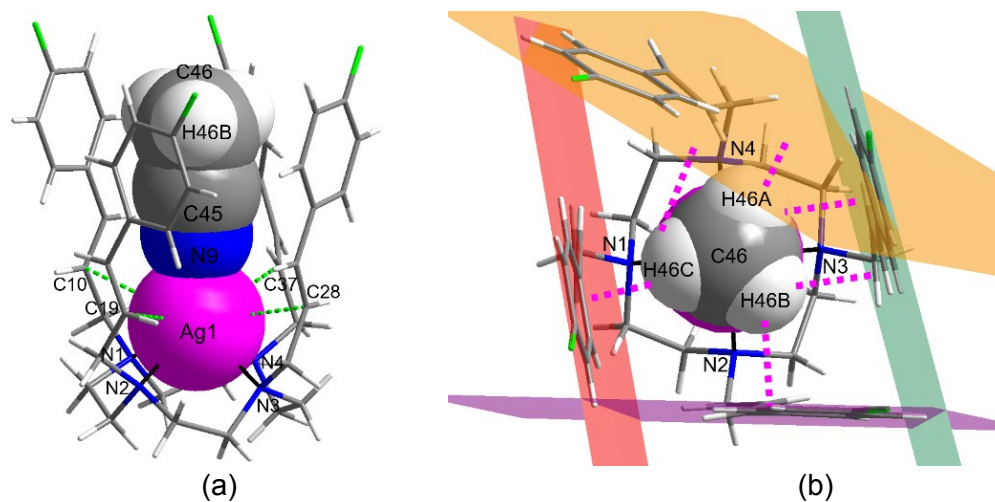


**Fig. S10** X-ray structure of **2c**/ $\text{AgCF}_3\text{SO}_3$ : (a) side view showing  $\text{Ag}^+$ – $\pi$  interaction (green dotted line) and (b) top view showing  $\text{H}_{\text{acetonitrile}}$ –benzene plane distances (pink dotted line). Difference-map plots show that the acetonitrile methyl H atoms are correctly oriented. Non-coordinated anions are omitted.

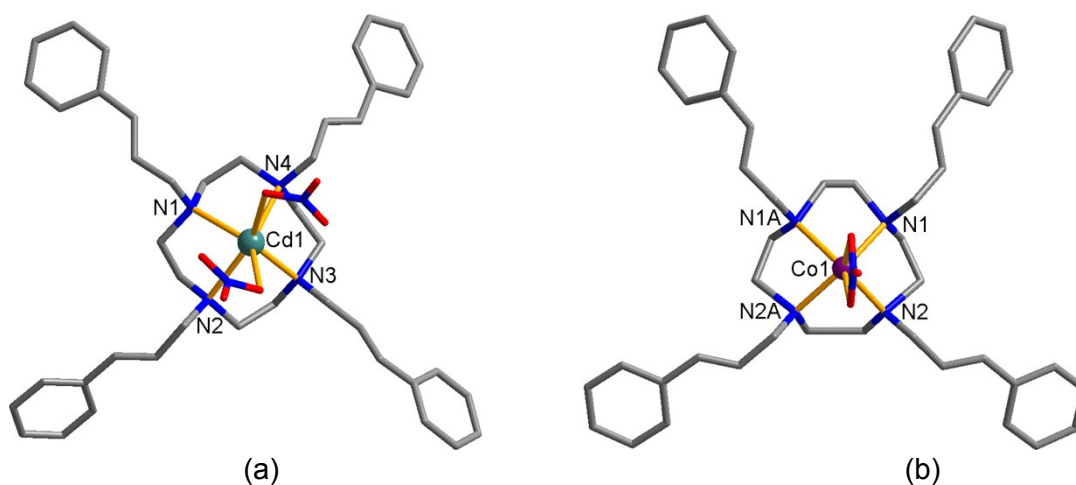


**Fig. S11** X-ray structure of (a) **2a**/ $\text{Cd}(\text{NO}_3)_2$  and (b) **2a**/ $\text{Co}(\text{NO}_3)_2$ . Hydrogen atoms and non-coordinated anion are omitted. Compound **2a**/ $\text{Co}^{2+}$  lies across a mirror plane.

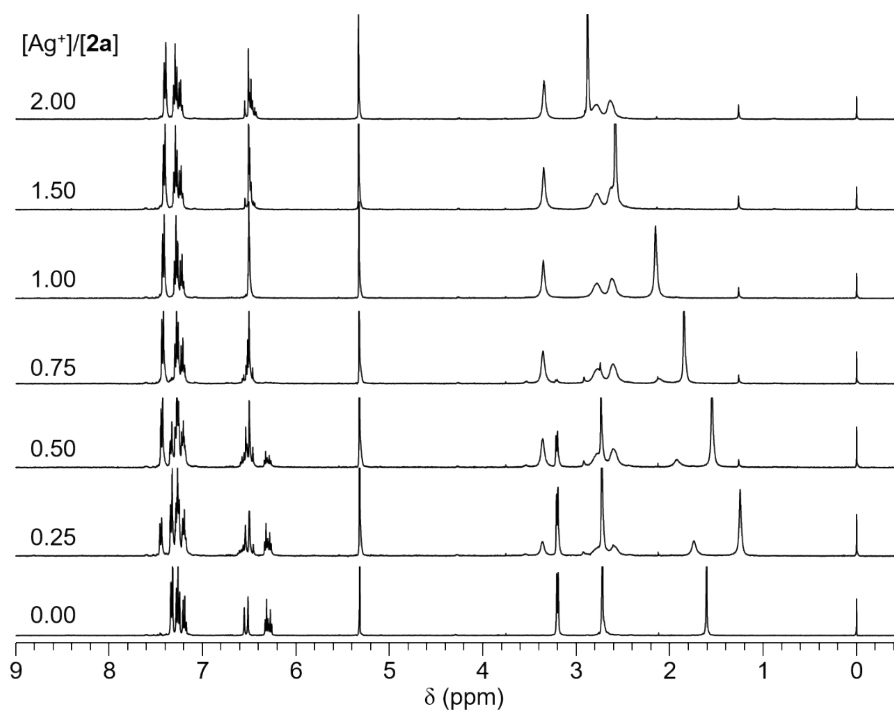


**Fig. S12**  $\text{Ag}^+$  ion-induced  $^1\text{H}$  NMR spectral changes of **2a** in a mixture of  $\text{CD}_2\text{Cl}_2$  and  $\text{CD}_3\text{OD}$ .

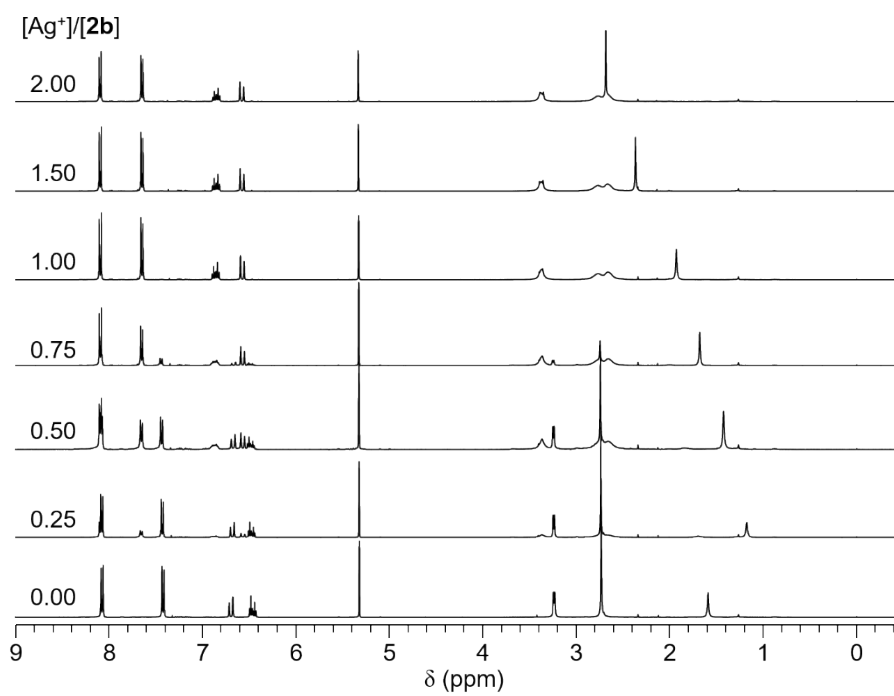


**Fig. S13**  $\text{Ag}^+$  ion-induced  $^1\text{H}$  NMR spectral changes of **2b** in a mixture of  $\text{CD}_2\text{Cl}_2$  and  $\text{CD}_3\text{OD}$ .

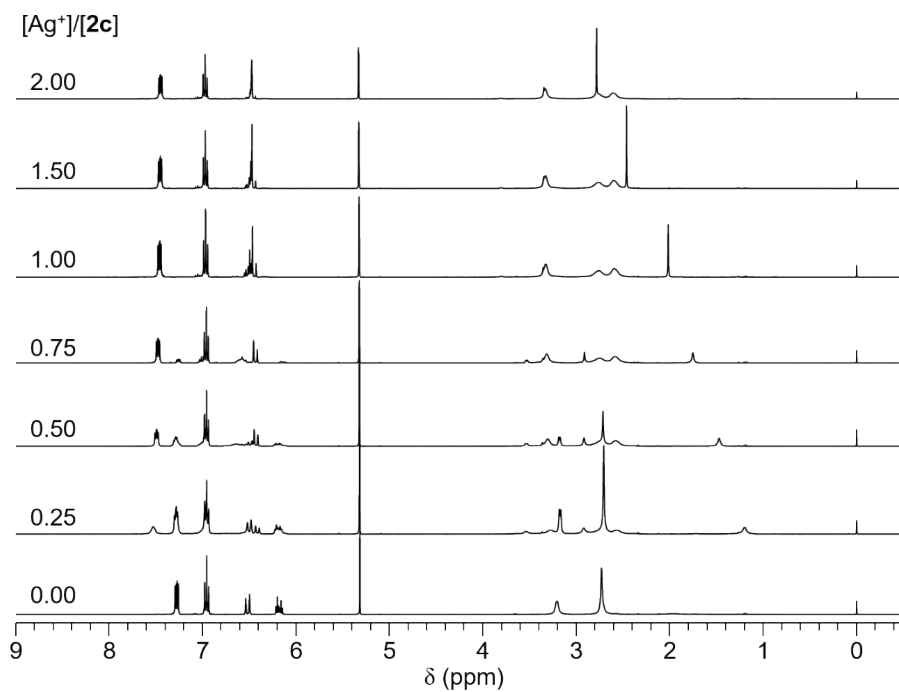


**Fig. S14**  $\text{Ag}^+$  ion-induced  $^1\text{H}$  NMR spectral changes of **2c** in a mixture of  $\text{CD}_2\text{Cl}_2$  and  $\text{CD}_3\text{OD}$ .

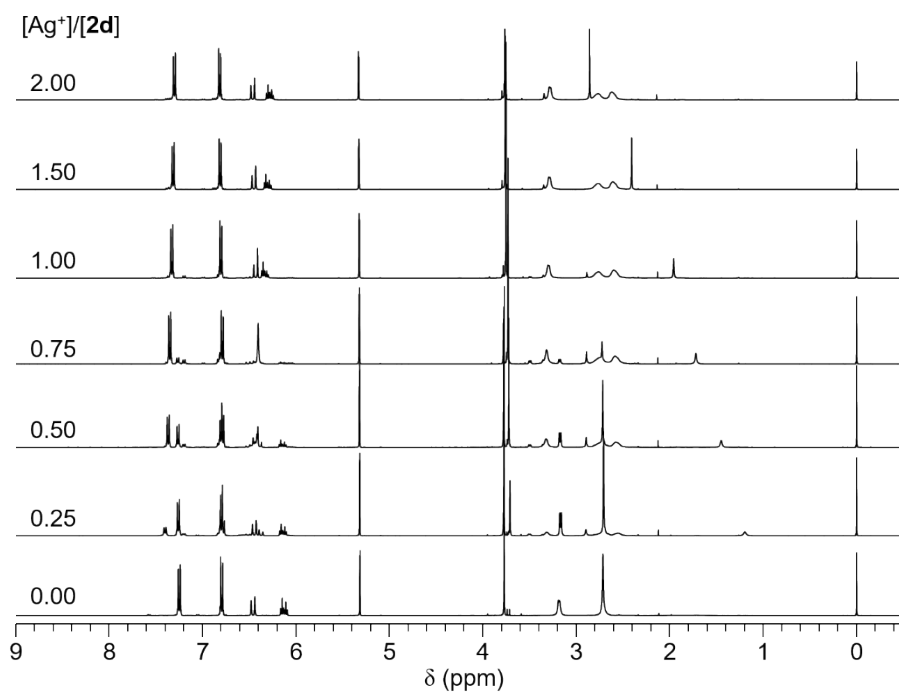


**Fig. S15**  $\text{Ag}^+$  ion-induced  $^1\text{H}$  NMR spectral changes of **2d** in a mixture of  $\text{CD}_2\text{Cl}_2$  and  $\text{CD}_3\text{OD}$ .

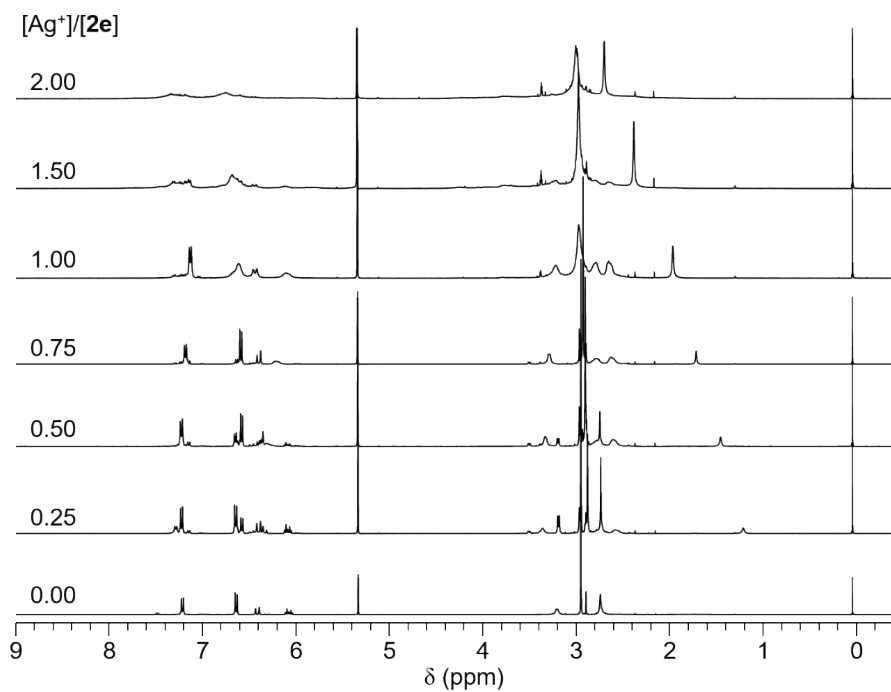


**Fig. S16**  $\text{Ag}^+$  ion-induced  $^1\text{H}$  NMR spectral changes of **2e** in a mixture of  $\text{CD}_2\text{Cl}_2$  and  $\text{CD}_3\text{OD}$ .

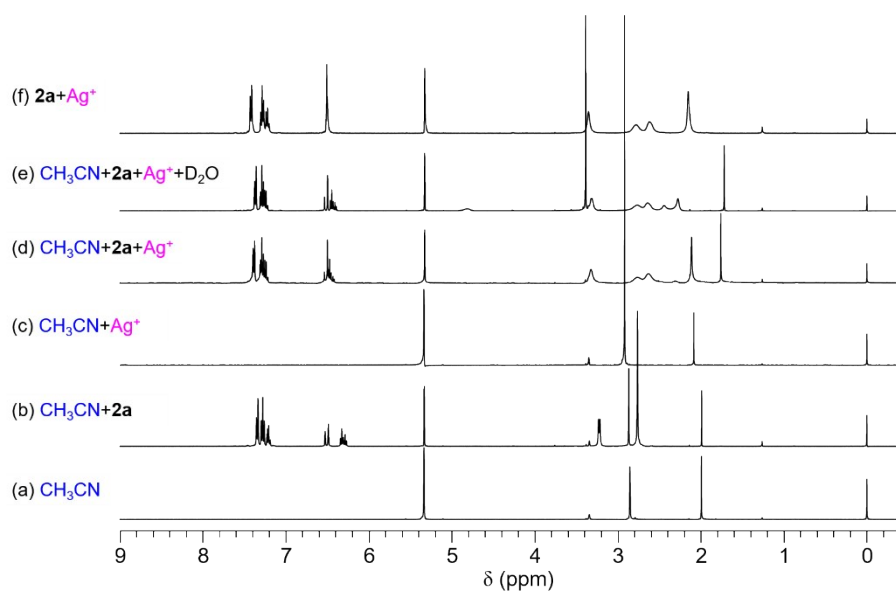


**Fig. S17** Comparative  $^1\text{H}$  NMR spectra of (a)  $\text{CH}_3\text{CN}$ , (b)  $\text{CH}_3\text{CN}+2\mathbf{a}$ , (c)  $\text{CH}_3\text{CN}+\text{Ag}^+$ , (d)  $\text{CH}_3\text{CN}+2\mathbf{a}+\text{Ag}^+$ , (e)  $\text{CH}_3\text{CN}+2\mathbf{a}+\text{Ag}^++\text{D}_2\text{O}$  and (f)  $2\mathbf{a}+\text{Ag}^+$  in a mixture of  $\text{CD}_2\text{Cl}_2$  and  $\text{CD}_3\text{OD}$ .

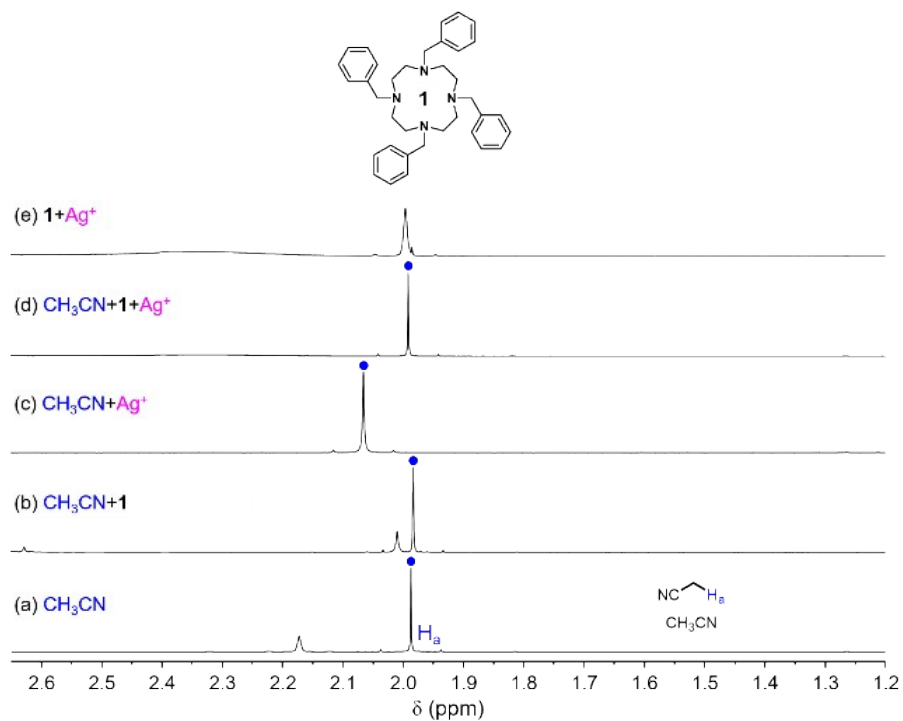


**Fig. S18** Comparative <sup>1</sup>H NMR spectra of (a) CH<sub>3</sub>CN, (b) CH<sub>3</sub>CN+**1**, (c) CH<sub>3</sub>CN+Ag<sup>+</sup>, (d) CH<sub>3</sub>CN+**1**+Ag<sup>+</sup> and (e) **1**+Ag<sup>+</sup> in a mixture of CD<sub>2</sub>Cl<sub>2</sub> and CD<sub>3</sub>OD.

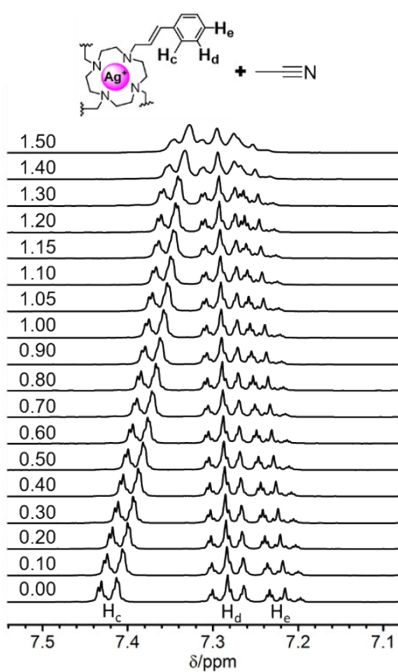


**Fig. S19** Acetonitrile-induced <sup>1</sup>H NMR spectral changes of **2a**/Ag<sup>+</sup> complex in a mixture of CD<sub>2</sub>Cl<sub>2</sub> and CD<sub>3</sub>OD.



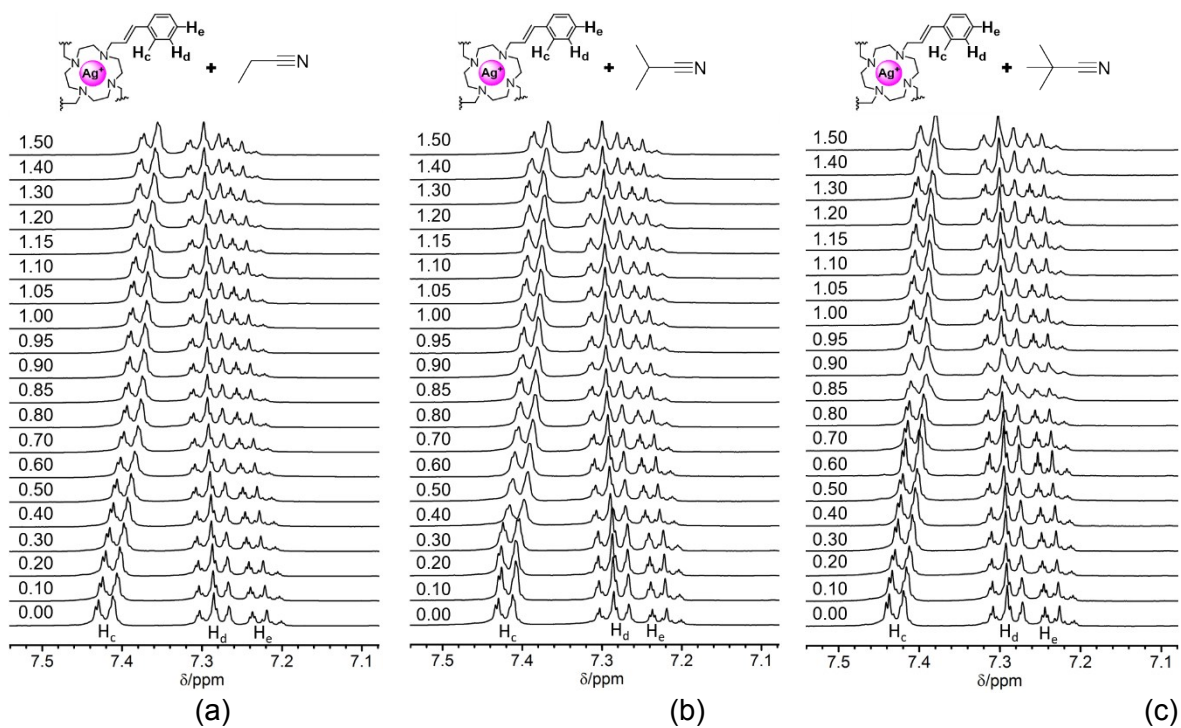


**Fig. S20** Bulky nitrile-induced  $^1\text{H}$  NMR spectral changes of  $2\text{a}/\text{Ag}^+$  complex in a mixture of  $\text{CD}_2\text{Cl}_2$  and  $\text{CD}_3\text{OD}$ : (a) propionitrile, (b) isobutyronitrile and (c) pivalonitrile.

**Table S2** Stability constants for the complexations of acetonitrile and bulky nitrile guests with  $2\text{a}/\text{Ag}^+$  complex

Acetonitrile	Bulky Nitrile		
	Propionitrile	Isobutyronitrile	Pivalonitrile
2.1(1)	1.9(1)	1.7(1)	1.7(1)

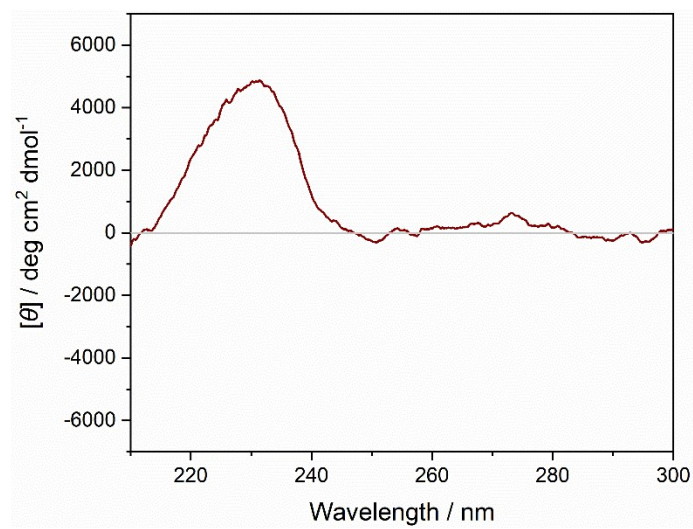
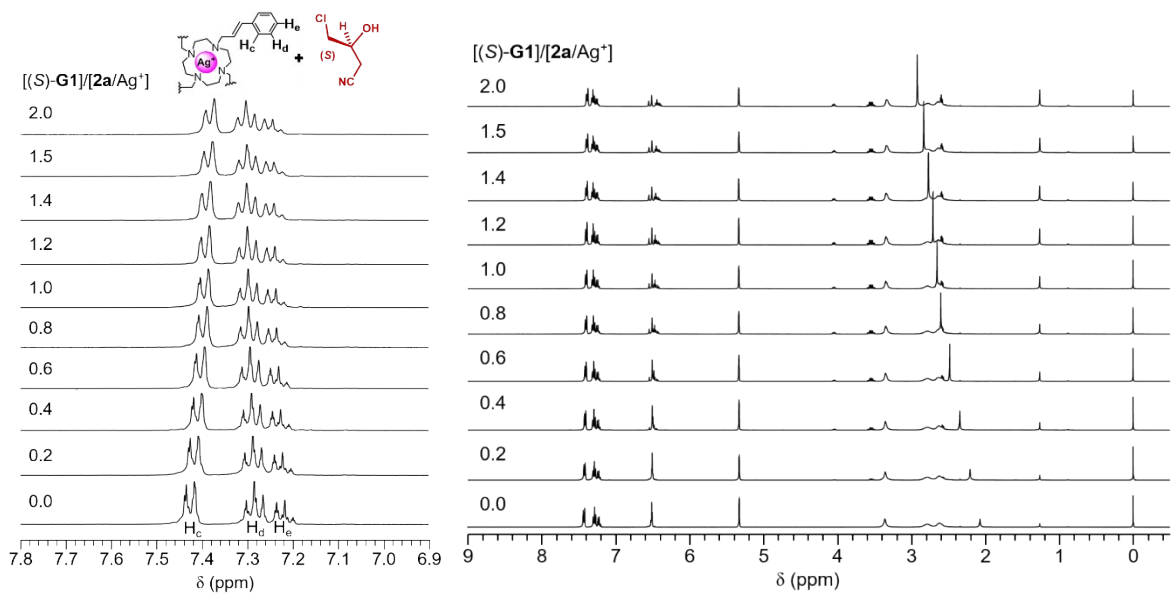
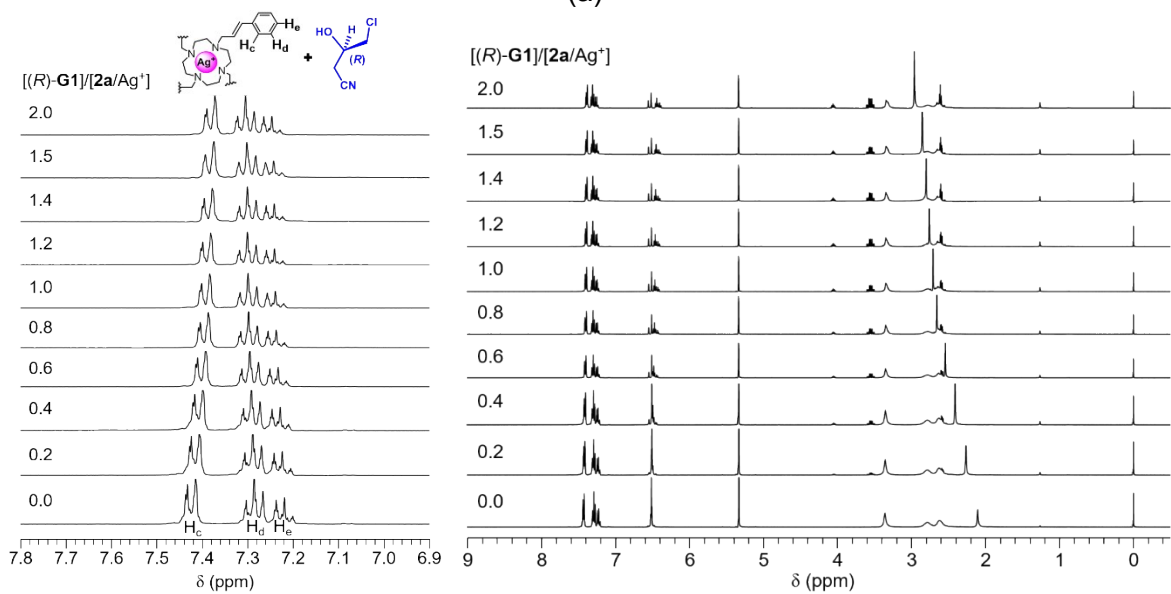


**Fig. S21** CD spectrum of chiral cyanohydrin (**G6**) ( $3.00 \times 10^{-3}\text{M}$ ) in the EtOH/1,4-dioxane (9/1) solution.



(a)



(b)

**Fig. S22** (a) (S)-G1 and (b) (R)-G1-induced <sup>1</sup>H NMR spectral changes in CD<sub>2</sub>Cl<sub>2</sub>/CD<sub>3</sub>OD.

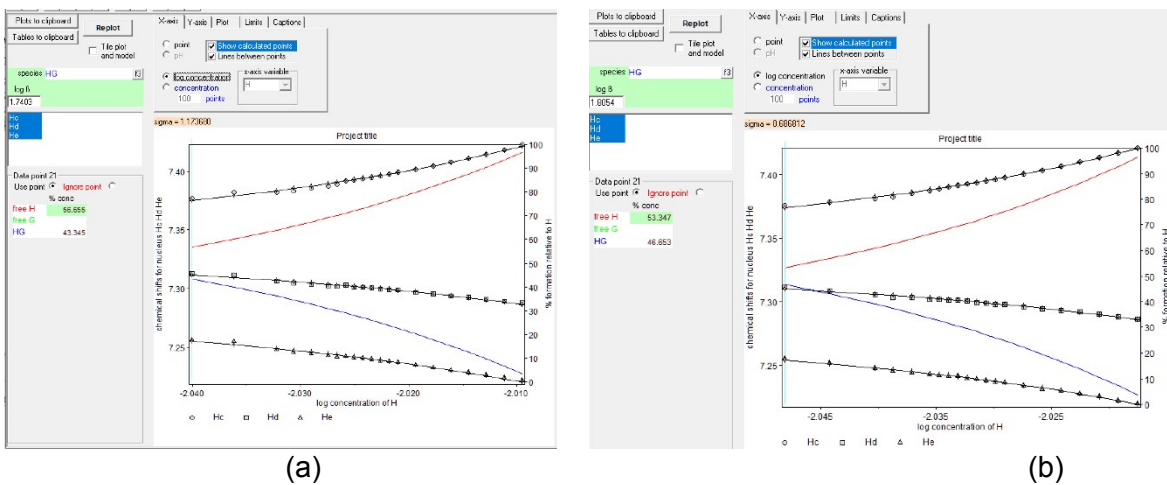


**Fig. S23** HyperNMR output for **2a**/ $\text{Ag}^+$  complex solution with (a) (*S*)-**G1** and (b) (*R*)-**G1**.

The DOSY NMR spectrum of **2a**/ $\text{Ag}^+$  and (*S*)-**G1** (Fig. S22) revealed the presence of only one species in a solution for each substance. The experimental diffusion coefficient derived from the spectra measured in  $\text{CD}_2\text{Cl}_2/\text{CD}_3\text{OD}$  at 233 K was  $7.08 \times 10^{-10} \text{ m}^2/\text{s}$ .

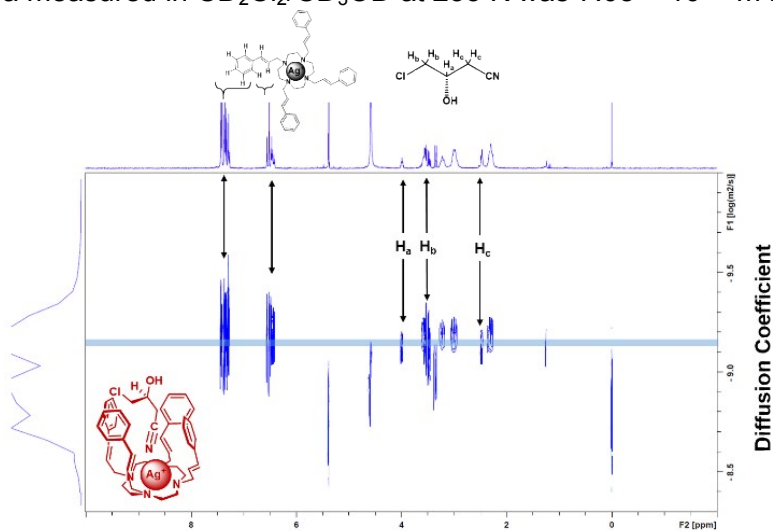


**Fig. S24** Diffusion-ordered spectroscopy (DOSY) of **2a**/ $\text{Ag}^+$  and (*S*)-**G1** in  $\text{CD}_2\text{Cl}_2/\text{CD}_3\text{OD}$  at 233K.

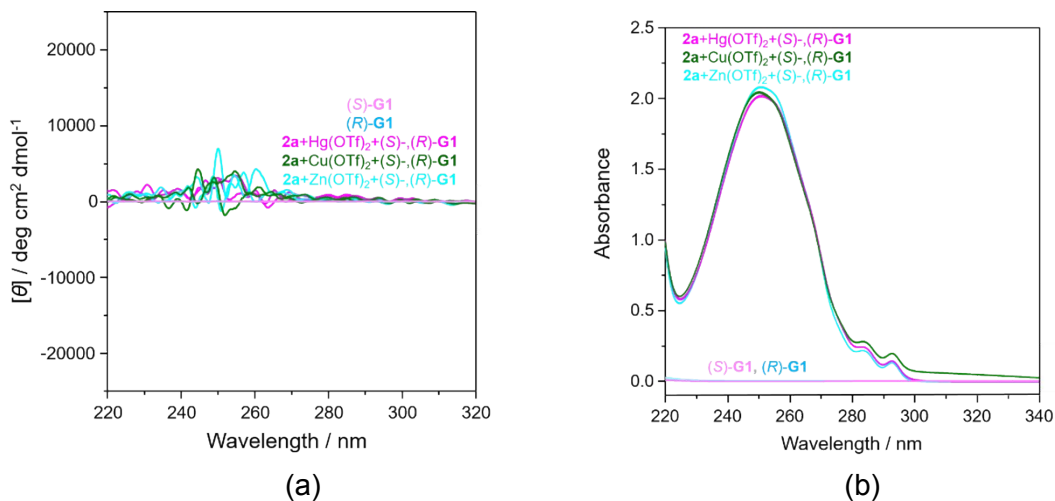


**Fig. S25** Guest-induced (a) CD and (b) UV-vis spectral changes for **2a** and another metal solutions.

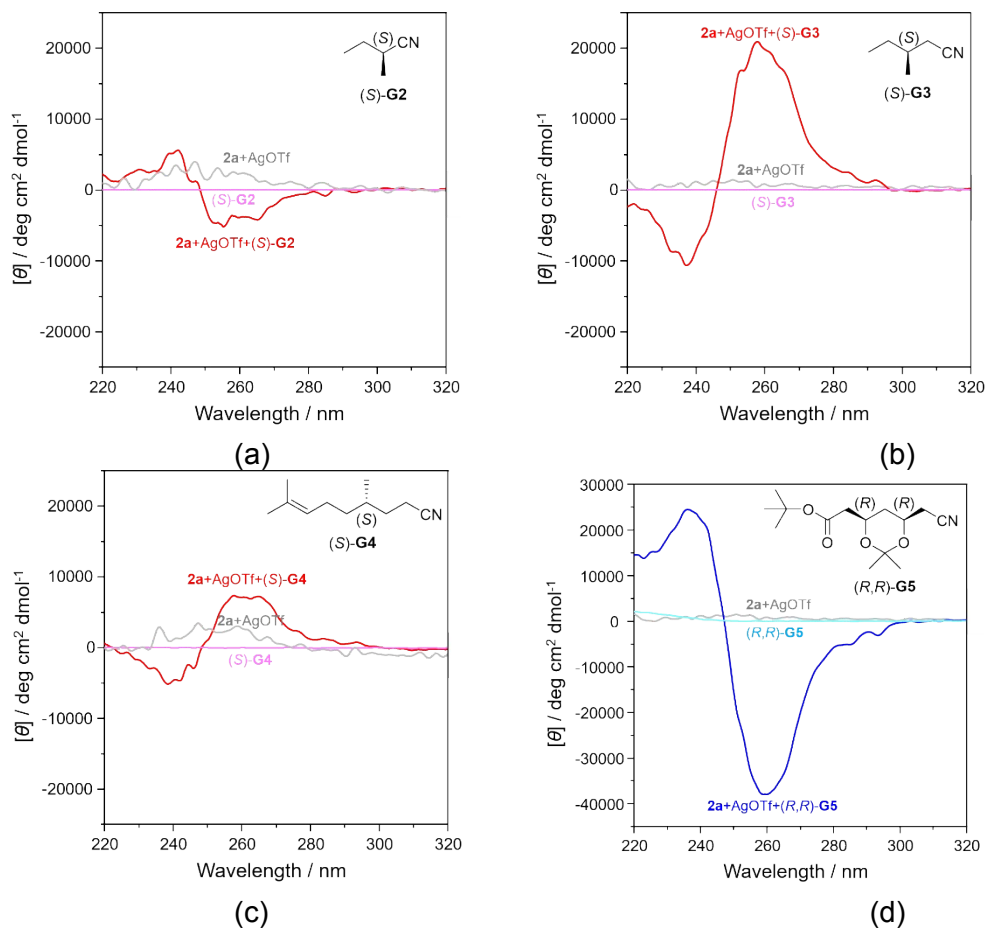


**Fig. S26** Chiral nitriles-induced CD spectral changes of **2a/Ag<sup>+</sup>** complex: (a) (S)-G2, (b) (S)-G3, (c) (S)-G4 and (d) (R,R)-G5 ( $[G] = 30.0 \times 10^{-3} \text{ M}$ ,  $[2a] = [AgOTf] = 3.00 \times 10^{-3} \text{ M}$ ).

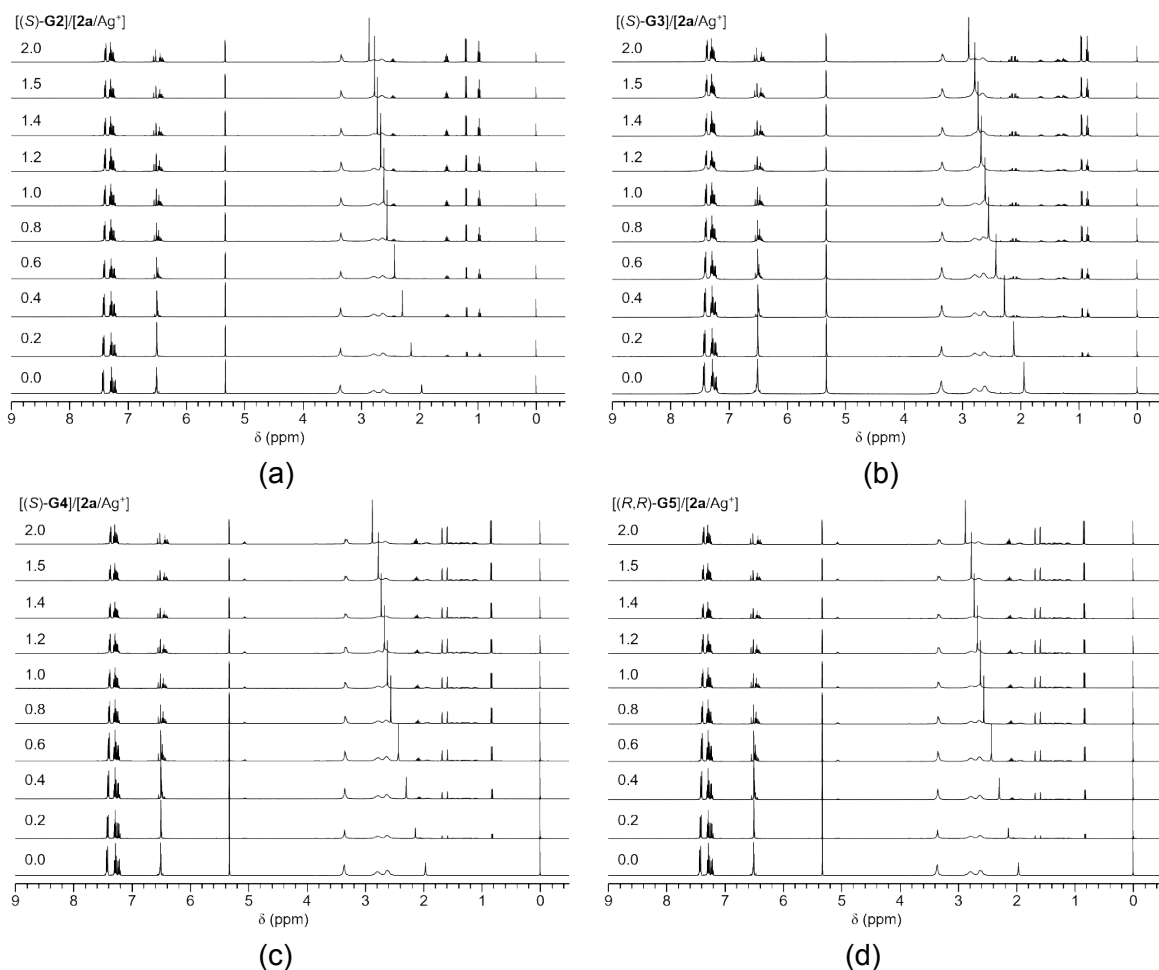
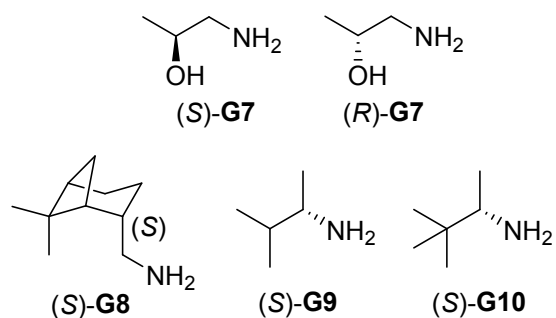


**Fig. S27** Chiral nitrile-induced  $^1\text{H}$  NMR spectral changes of  $2\mathbf{a}/\text{Ag}^+$  complex in a mixture of  $\text{CD}_2\text{Cl}_2$  and  $\text{CD}_3\text{OD}$ : (a) (S)-**G2**, (b) (S)-**G3**, (c) (S)-**G4** and (d) (R,R)-**G5**.

When (R,R)-**G5** was examined under the same conditions (Fig. S26), initial negative and then positive Cotton effects were observed. The  $\log K$  values of the interactions between the  $2\mathbf{a}/\text{Ag}^+$  complex with chiral guests **G2–G5** were in the range of 1.5–1.9 (Fig. S27 and Table S3).

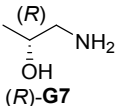
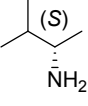
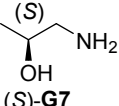
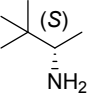
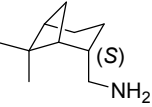
**Table S3** Stability constants for the complexations of chiral nitrile guests with  $2\mathbf{a}/\text{Ag}^+$  complex

Chiral Nitrile					
(R)- <b>G1</b>	(S)- <b>G1</b>	(S)- <b>G2</b>	(S)- <b>G3</b>	(S)- <b>G4</b>	(R,R)- <b>G5</b>
1.8(5)	1.7(3)	1.7(1)	1.6(1)	1.9(1)	1.5(1)



**Fig. S28** Structure of chiral amines as a guest (**G7-G10**).

**Table S4**  $[\alpha]_D$  of chiral alkyl amines

Compound	Temp. (°C)	$[\alpha]_D$	Compound	Temp. (°C)	$[\alpha]_D$
 (R)-G7	20	-25.8 (c 1.8, EtOH) <sup>S5</sup>	 (S)-G9	22	+3.7 (c 0.3, H <sub>2</sub> O) <sup>S8</sup>
 (S)-G7	22	44.4 (c 1, MeOH) <sup>S6</sup>	 (S)-G10	20	+18.1 (c 2.15, MeOH) <sup>S9</sup>
 (S)-G8	26	-27.9 (neat) <sup>S7</sup>			

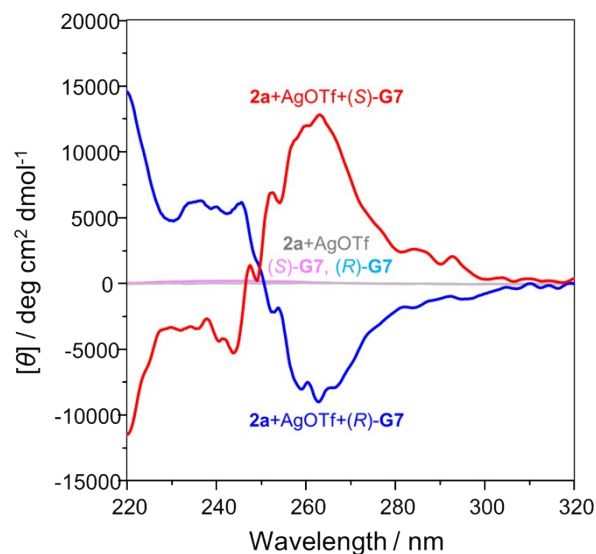


**Fig. S29** CD spectra ( $[G] = 30.0 \times 10^{-3} \text{ M}$ ,  $[2a] = [AgOTf] = 3.00 \times 10^{-3} \text{ M}$ ) of  $2a/Ag^+$  complex, chiral **G7** and chiral **G7@2a/Ag<sup>+</sup>** in the mixed solvent (EtOH/1,4-dioxane = 9:1).

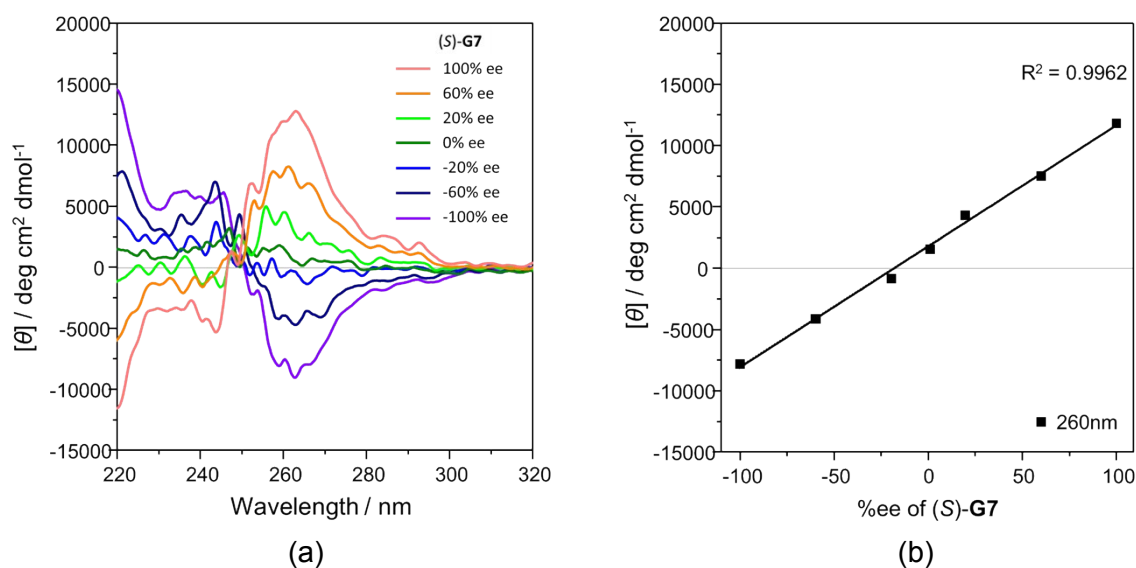


**Fig. S30** (a) CD spectra (EtOH/1,4-dioxane, 273 K,  $[2a/Ag^+] = 3.00 \times 10^{-3} \text{ M}$ ) of  $2a/Ag^+$  in presence of **G7** ( $30.0 \times 10^{-3} \text{ M}$ ) with various ee values and (b) the corresponding ee calibration plots at 260 nm.



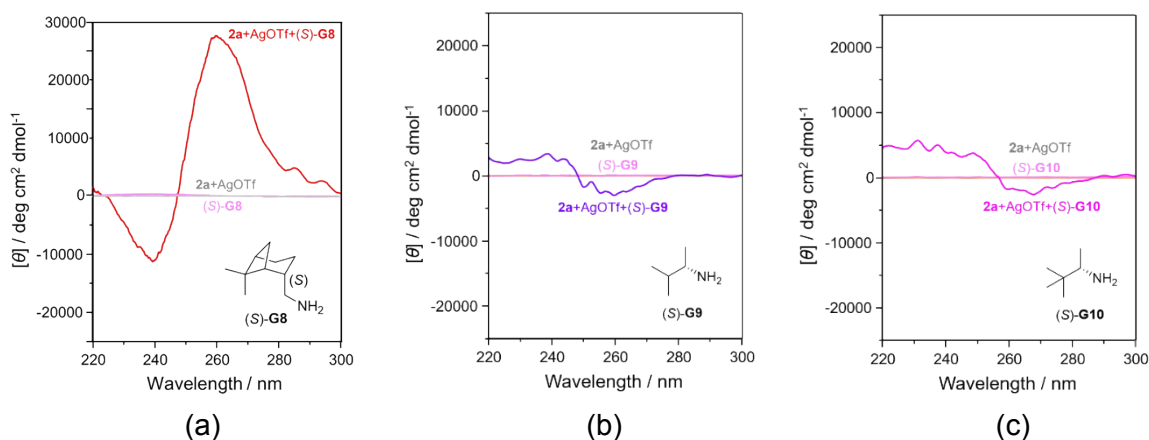


**Fig. S31** Chiral amines-induced CD spectral changes of **2a**/ $\text{Ag}^+$  complex: (a) (S)-**G8**, (b) (S)-**G9** and (c) (S)-**G10** ( $[\text{G}] = 30.0 \times 10^{-3} \text{ M}$ ,  $[\text{2a}] = [\text{AgOTf}] = 3.00 \times 10^{-3} \text{ M}$ ).

## References

- S1 X. Q. Li, Y. X. Yang, W. L. Wang, B. Hu, H. M. Xue, T. Y. Zhang and X. T. Zhang, *Chin. Chem. Lett.*, 2011, **22**, 765-767.
- S2 C. Jiang and H. Hong, *Lett. Org. Chem.*, 2012, **9**, 520-521.
- S3 P. L. Brewer, D. E. Butler, C. F. Deering, T. V. Le, A. Millar, T. N. Nanninga and B. D. Roth, *Tetrahedron Lett.*, 1992, **33**, 2279-2282.
- S4 Y.-C. Zheng, J.-H. Xu, H. Wang, G.-Q. Lin, R. Hong and H.-L. Yu, *Adv. Synth. Catal.*, 2017, **359**, 1185-1193.
- S5 M. A. Gray, L. Konopski and Y. Langlois, *Synth. Commun.*, 1994, **24**, 1381-1387.
- S6 Tokyo University of Science Educational Foundation Administrative Organization-US2011/319650, 2011, A1.
- S7 H. C. Brown, W. R. Heydkamp, Eli. Breuer and W. S. Murphy, *J. Am. Chem. Soc.*, 1964, **86**, 3565-3566.
- S8 P. C. J. Kamer, M. C. Cleij, R. J. M. Nolle, T. Harada, A. M. F. Hezemans and W. Drenth, *J. Am. Chem. Soc.*, 1988, **110**, 1581-1587.
- S9 M. C. Schopohl, A. Faust, D. Mirk, R. Fröhlich, O. Kataeva and S. R. Waldvogel, *Eur. J. Org. Chem.*, 2005, 2987-2999.

**Table S5** Crystallographic Data and Structure Refinement

	<b>2a</b>	<b>2a/Ag</b>	<b>2a/Cd</b>	<b>2a/Co</b>	<b>2b/Ag</b>
formula	C <sub>44</sub> H <sub>52</sub> N <sub>4</sub>	C <sub>46</sub> H <sub>55</sub> AgF <sub>6</sub> N <sub>5</sub> P	C <sub>46</sub> H <sub>56</sub> CdCl <sub>2</sub> N <sub>6</sub> O <sub>6</sub>	C <sub>44</sub> H <sub>52</sub> CoN <sub>6</sub> O <sub>6</sub>	C <sub>47</sub> H <sub>51</sub> AgF <sub>3</sub> N <sub>9</sub> O <sub>11</sub> S
formula weight	636.90	930.79	972.26	819.84	1114.90
Temperature (K)	150	120(2)	120(2)	120(2)	120(2)
crystal system	Triclinic	Monoclinic	Monoclinic	Orthorhombic	Triclinic
space group	<i>P</i> -1	<i>P</i> 2 <sub>1</sub> / <i>n</i>	<i>P</i> 2 <sub>1</sub> / <i>c</i>	<i>Pnma</i>	<i>P</i> -1
<i>Z</i>	1	4	4	4	2
<i>a</i> (Å)	8.1561(4)	9.8867(6)	18.948(3)	17.4039(10)	13.6723(5)
<i>b</i> (Å)	9.8581(5)	43.590(2)	26.442(4)	28.4415(16)	13.6784(5)
<i>c</i> (Å)	12.6906(7)	10.0840(6)	9.0080(13)	8.1734(4)	14.1978(5)
$\alpha$ (°)	67.2140(10)	90	90	90	71.0716(5)
$\beta$ (°)	81.5070(10)	91.9702(12)	91.789(2)	90	86.9270(6)
$\gamma$ (°)	80.4560(10)	90	90	90	89.7603(6)
<i>V</i> (Å <sup>3</sup> )	923.80(8)	4343.2(4)	4511.2(12)	4045.8(4)	2507.77(16)
<i>D</i> <sub>calc</sub> (g/cm <sup>3</sup> )	1.145	1.423	1.432	1.346	1.476
$\mu$ (mm <sup>-1</sup> )	0.067	0.566	0.657	0.481	0.523
2 $\theta$ <sub>max</sub> (°)	52	52	52	52	52
reflections collected	5313	25251	38044	22297	30173
independent	3609	8539	8874	4057	9840
reflections	[ <i>R</i> <sub>int</sub> = 0.0112]	[ <i>R</i> <sub>int</sub> = 0.0715]	[ <i>R</i> <sub>int</sub> = 0.1233]	[ <i>R</i> <sub>int</sub> = 0.0596]	[ <i>R</i> <sub>int</sub> = 0.0448]
goodness-of-fit on <i>F</i> <sup>2</sup>	1.013	1.016	1.015	1.035	1.021
<i>R</i> <sub>1</sub> , <i>wR</i> <sub>2</sub> [ <i>I</i> > 2 $\sigma$ ( <i>I</i> )]	0.0395, 0.1070	0.0447, 0.0976	0.0668, 0.1608	0.0429, 0.1085	0.0493, 0.1306
<i>R</i> <sub>1</sub> , <i>wR</i> <sub>2</sub> [all data]	0.0486, 0.1159	0.0678, 0.1160	0.1172, 0.2008	0.0569, 0.1181	0.0579, 0.1384

	<b>2c/Ag</b>	<b>2d</b>	<b>2e</b>
formula	C <sub>47</sub> H <sub>51</sub> AgF <sub>7</sub> N <sub>5</sub> O <sub>3</sub> S	C <sub>48</sub> H <sub>60</sub> N <sub>4</sub> O <sub>4</sub>	C <sub>52</sub> H <sub>72</sub> N <sub>8</sub>
formula weight	1006.85	757.00	809.17
Temperature (K)	120(2)	120(2)	120(2)
crystal system	Triclinic	Triclinic	Tetragonal
space group	<i>P</i> -1	<i>P</i> -1	<i>P</i> -4
<i>Z</i>	2	1	4
<i>a</i> (Å)	10.0234(3)	9.370(6)	17.703(2)
<i>b</i> (Å)	10.3546(3)	9.873(6)	17.703(2)
<i>c</i> (Å)	22.0904(7)	12.853(8)	14.619(3)
$\alpha$ (°)	97.2008(4)	101.209(10)	90
$\beta$ (°)	95.9244(5)	110.101(10)	90
$\gamma$ (°)	92.3991(5)	100.626(10)	90
<i>V</i> (Å <sup>3</sup> )	2259.00(12)	1053.8(12)	4581.5(14)
<i>D</i> <sub>calc</sub> (g/cm <sup>3</sup> )	1.480	1.193	1.173
$\mu$ (mm <sup>-1</sup> )	0.568	0.076	0.070
$2\theta_{\max}$ (°)	52	52	52
reflections collected	26629	12267	26843
independent	8885	4141	9016
reflections	[ <i>R</i> <sub>int</sub> = 0.0257]	[ <i>R</i> <sub>int</sub> = 0.0952]	[ <i>R</i> <sub>int</sub> = 0.1881]
goodness-of-fit on <i>F</i> <sup>2</sup>	1.043	0.980	1.030
<i>R</i> <sub>1</sub> , <i>wR</i> <sub>2</sub> [ <i>I</i> > 2 $\sigma$ ( <i>I</i> )]	0.0260, 0.0672	0.0729, 0.1754	0.0990, 0.2147
<i>R</i> <sub>1</sub> , <i>wR</i> <sub>2</sub> [all data]	0.0294, 0.0741	0.1112, 0.2064	0.02344, 0.2843

**Table S6** Selected Bond Lengths (Å) and Bond Angles (°) for **2a/Ag**

Ag1-N1	2.486(3)	Ag1-N2	2.488(3)
Ag1-N3	2.480(3)	Ag1-N4	2.491(3)
Ag1-N5	2.226(3)		
N1-Ag1-N2	75.72(10)	N1-Ag1-N3	118.36(9)
N1-Ag1-N4	74.45(10)	N1-Ag1-N5	121.21(10)
N2-Ag1-N3	74.71(10)	N2-Ag1-N4	119.08(10)
N2-Ag1-N5	120.61(11)	N3-Ag1-N4	74.90(10)
N3-Ag1-N5	120.42(10)	N4-Ag1-N5	120.31(11)

**Table S7** Selected Bond Lengths (Å) and Bond Angles (°) for **2a/Cd**

Cd1-N1	2.374(5)	Cd1-N2	2.510(5)
Cd1-N3	2.375(5)	Cd1-N4	2.497(6)
Cd1-O2	2.363(4)	Cd1-O4	2.405(5)
N1-Cd1-N2	75.17(18)	N1-Cd1-N3	121.23(18)
N1-Cd1-N4	75.4(2)	N1-Cd1-O2	132.56(18)
N1-Cd1-O4	96.56(17)	N2-Cd1-N3	75.40(17)
N2-Cd1-N4	120.11(18)	N2-Cd1-O2	84.32(18)
N2-Cd1-O4	151.85(17)	N3-Cd1-N4	77.3(2)
N3-Cd1-O2	93.01(17)	N3-Cd1-O4	129.64(17)
N4-Cd1-O2	149.29(18)	N4-Cd1-O4	82.22(18)
O2-Cd1-O4	81.92(17)		

**Table S8** Selected Bond Lengths (Å) and Bond Angles (°) for **2a/Co**

Co1-N1	2.187(2)	Co1-N2	2.207(2)
Co1-O1	2.138(2)	Co1-O2	2.174(2)
N1-Co1-N2	80.16(8)	N1-Co1-N1A	82.05(11)
N1-Co1-N2A	132.86(8)	N1-Co1-O1	131.27(6)
N1-Co1-O2	91.21(7)	N2-Co1-N2A	80.82(13)
N2-Co1-O1	92.07(7)	N2-Co1-O2	132.28(7)
O1-Co1-O2	59.37(9)		

**Table S9** Selected Bond Lengths (Å) and Bond Angles (°) for **2b/Ag**

Ag1-N1	2.460(3)	Ag1-N2	2.479(3)
Ag1-N3	2.495(3)	Ag1-N4	2.536(3)
Ag1-N9	2.224(3)		
N1-Ag1-N2	74.64(9)	N1-Ag1-N3	117.55(9)
N1-Ag1-N4	75.26(10)	N1-Ag1-N9	116.35(10)
N2-Ag1-N3	73.70(10)	N2-Ag1-N4	117.46(9)
N2-Ag1-N9	124.04(10)	N3-Ag1-N4	73.98(10)
N3-Ag1-N9	126.04(10)	N4-Ag1-N9	118.36(10)

**Table S10** Selected Bond Lengths (Å) and Bond Angles (°) for **2c/Ag**

Ag1-N1	2.4753(15)	Ag1-N2	2.4721(15)
Ag1-N3	2.4933(15)	Ag1-N4	2.5283(16)
Ag1-N5	2.2253(17)		
N1-Ag1-N2	76.11(5)	N1-Ag1-N3	117.94(5)
N1-Ag1-N4	74.80(5)	N1-Ag1-N5	119.03(6)
N2-Ag1-N3	74.12(5)	N2-Ag1-N4	117.79(5)
N2-Ag1-N5	121.06(6)	N3-Ag1-N4	73.25(5)
N3-Ag1-N5	123.01(6)	N4-Ag1-N5	121.14(6)